IEEE Access
Multidisciplinary | Rapid Review | Open Access Journal

Received 2 March 2024, accepted 11 March 2024, date of publication 18 March 2024, date of current version 22 March 2024.

Digital Object Identifier 10.1109/ACCESS.2024.3377111

RESEARCH ARTICLE

Sensor Fusion and Machine Learning for Seated Movement Detection With Trunk Orthosis

AHMAD ZAHID RAO[1], SABA SHAHID SIDDIQUE[1], MUHAMMAD DANISH MUJIB[1], MUHAMMAD ABUL HASAN[1,2], AHMAD O. ALOKAILY[3,4], AND TAYYABA TAHIRA[5]

[1]Department of Biomedical Engineering, NED University of Engineering and Technology, Karachi 75270, Pakistan
[2]Neurocomputation Laboratory, National Center of Artificial Intelligence, Karachi 75270, Pakistan
[3]Department of Biomedical Technology, College of Applied Medical Sciences, King Saud University, Riyadh 11495, Saudi Arabia
[4]King Salman Center for Disability Research, Riyadh 11614, Saudi Arabia
[5]Operative Dentistry and Endodontics Department, Dow International Dental College, Dow University of Health Sciences, Karachi 74200, Pakistan

Corresponding authors: Ahmad Zahid Rao (ahmadrao@neduet.edu.pk) and Ahmad O. Alokaily (aalokaily@ksu.edu.sa)

This work was supported by the King Salman Center for Disability Research for funding this work through Research Group under Grant KSRG-2023-299.

This work involved human subjects or animals in its research. Approval of all ethical and experimental procedures and protocols was granted by the Research Ethics Committee of NED University of Engineering and Technology under Approval No. ASRB/878, and performed in line with the Declaration of Helsinki.

ABSTRACT Advanced assistive devices developed for activities of daily living use machine learning (ML) for motion intention detection using wearable sensors. Trunk assistive devices provide safety, balance, and independence for wheelchair users individuals who spend prolonged hours in sitting positions. We used ML for trunk movement intention detection with a trunk orthosis. Sensor fusion technique with four electromyography (EMG) and one inertial measurement unit (IMU) sensor signals are used to develop a three-level classification system. Forty participants engaged in seated trunk movement trials wearing the orthosis. The trials comprised 30 movements involving trunk flexion/extension, lateral bending, and axial rotation. The wrapper method was used to reduce essential EMG features. Ensemble (ES), k-nearest neighbors (KNN), and support vector machine ML classifiers were used. Twenty-six features (five EMG for each of four muscles and six for IMU) were used to develop ten individual ML models, resulting in an average accuracy of 95.44%. Eight models achieved the highest accuracy with the ES and two with KNN. The models were then cascaded to form a trunk motion detection system that achieved a test accuracy of 87.0%. The promising result of this study can be implemented for trunk motion recognition with active trunk orthosis.

INDEX TERMS Electromyography (EMG), fall, IMU, intention, machine learning, movement, seated, sensor fusion, trunk.

I. INTRODUCTION

Prolonged sitting of more than ten hours on a daily basis is common among wheelchair users [1]. To prevent the development of pressure sores, this prolonged sitting requires frequent trunk movements for posture adjustment to shift the person's weight multiple times per hour [2]. The trunk is an essential part of the kinematic chain that facilitates upper limb movements for individuals in a seated position [3]. Therefore, the daily life activities of wheelchair users rely on seated trunk movements as an indispensable component of their functional mobility. An unstable trunk leads to lower functional independence and a higher risk of accidental falls in seated reaching movements from a wheelchair [4], [5]. Trunk instability can be present in the elderly for whom movement disorders are common [6], [7], [8] especially because of their reduced control and strength during reaching movements [9], as well as in people with neuromuscular disorders because of their underlying condition [10].

Various trunk assistive devices can be used to enhance the seated mobility [11], [12], [13], [14]. However, these devices are limited in their ability to adjust the assistive force

The associate editor coordinating the review of this manuscript and approving it for publication was Md. Kafiul Islam.

dynamically according to user needs. To provide dynamic assistance and efficient interaction between the human and the device, it is important to be able to detect motion intention. Machine learning (ML) is a powerful tool that can be utilized to detect trunk motion and predict useful parameters. Trunk related studies that utilize ML techniques include those for fall prediction in the elderly [15], trunk muscle fatigue prediction [16], automatic detection of trunk compensatory movements during seated tasks [17], [18], scoliosis classification [19], low back pain classification and risk assessment [20], [21], [22], [23], and performance in sports [24].

A few studies involve the use of ML for the control of seated trunk assistive devices using electromyography (EMG) and inertial measurement unit (IMU) sensors. Two ML algorithms, the quadratic discriminant analysis and support vector machine (SVM), were used to classify 16 trunk movements [25]. An active postural support brace was worn while the participants made these seated trunk movements. Data from the IMU sensors was used to detect the movement intentions with accuracies of over 95%. Another study implemented ML on EMG data to identify trunk movements for the control of a spinal orthosis. The random forest, k-nearest neighbors (KNN), and SVM ML algorithms were used to distinguish between four daily movements and achieved accuracies of more than 88% [26]. Additionally, the sensor fusion technique [27] for combining EMG and IMU sensor data is known to improve the performance of ML predictions [28]. While it is commonly used for assistive devices of the upper [29] and lower limbs [30], [31], sensor fusion has not been applied to trunk assistive devices.

Therefore, this study aimed to utilize the sensor fusion technique with data from EMG and IMU sensors for trunk movement intention detection with the chair-mounted passive trunk orthosis (CMPTO). The objectives were to identify discriminative features, apply ML algorithms, select suitable ML models, and develop a predictive system that could classify 30 seated trunk movements. This system can be implemented in an active version of CMPTO that can assist trunk movements according to user intentions.

II. MATERIALS AND METHODS

A. PARTICIPANTS

Forty young, healthy males with an average age of 21.81 ± 3.13 SD years and an average body mass index of 22.92 ± 4.68 kg/m2 participated in this assessment. The research adhered to the principles of the Declaration of Helsinki and was approved by the Research Ethics Committee at the NED University of Engineering & Technology. Additionally, it followed specific exclusion criteria to account for the potential impact of the neurological or neuromuscular systems on movement. All participants provided written consent and were informed about the study' s design.

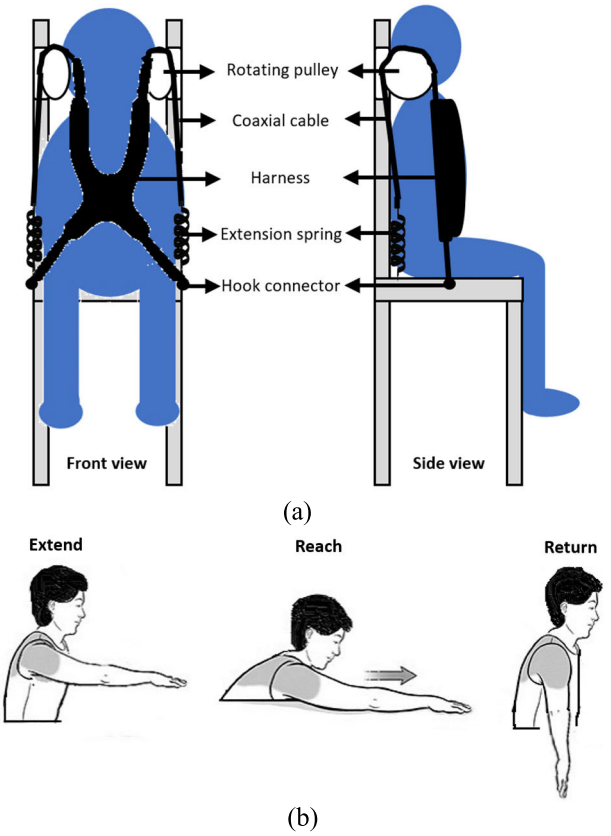

FIGURE 1. (a) Visual representation of the front and side views of the chair-mounted passive trunk orthosis. (b) The sequence of stages in each task: Extend, Reach, and Return.

B. EXPERIMENTAL PROCEDURE

Participants were fitted with the CMPTO (Figure 1a) while seated [32]. They were asked to perform ten distinct tasks that involved trunk flexion-extension (FE), lateral bending (LB), and axial rotation (AR). Each task involved three stages: (i) Extend, in which the upper limb extended towards the target with an unsupported upright trunk; (ii) Reach, involving maximal trunk sway from the neutral upright posture; and (iii) Return, involving returning to the resting upright position (Figure 1b).

All tasks were performed in a seated position across five horizontal orientations (0°, 45°, 90°, 135°, 180°) using both right and left upper limbs (Figure 2a). The tasks were carried out in a random order to avoid influencing the results and each participant conducted three trials, with a delay provided according to their preference to mitigate fatigue effects. The participants were given a familiarization session with the experimental procedure and were instructed to perform each movement to their maximum capability.

C. DATA COLLECTION

Figure 2b shows the IMU and EMG sensors on a participant's trunk. The IMU system (sampling frequency: 100 Hz; model:

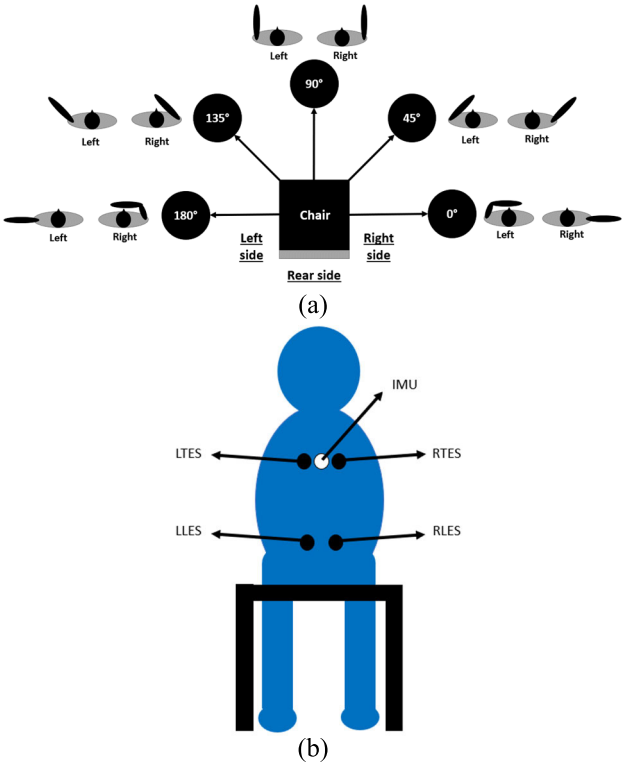

FIGURE 2. (a) Experimental setup (top view) showing the five horizontal orientations of target locations (0°, 45°, 90°, 135°, 180°) with respect to the subject's chair and the movements performed at each target with the right and left upper limbs. (b) Placement of one IMU (white) and four EMG (black) sensors on the participant's trunk (rear-view). The EMG sensors are labelled as RTES: Right Thoracic Erector Spinae, LTES: Left Thoracic Erector Spinae, RLES: Right Lumbar Erector Spinae, LLES: Left Lumbar Erector Spinae.

Awinda; manufacturer: Xsens, Enschede, The Netherlands; manufacture year: 2019) was used to capture kinematic data. A single IMU sensor was placed on the trunk midline at the T9 spinous process. Moreover, the EMG system (sampling frequency: 2048 Hz; model: Mobi; manufacturer: Twente Medical Systems International (TMSi), Oldenzaal, The Netherlands, manufacture year: 2016) was used to capture the muscle activity. The data from IMU and EMG sensors were synchronized in time, thus allowing for fusion of both sensor's data representing concurrent movement and muscle activity. The four muscles studied were the bilateral (right and left) thoracic erector spinae (TES) muscles, and the bilateral (right and left) lumbar erector spinae (LES) muscles. The electrodes for the TES muscles were located 3 cm bilaterally to the T9 spinous process and those for the LES muscles were located 3 cm bilaterally to the L4 spinous process. The ground electrode was placed over the right iliac crest, following the SENIAM guidelines.

D. DATA PREPROCESSING

We used a third-order Butterworth band-pass infinite impulse response filter for the preprocessing of EMG signals to eliminate the electrocardiography noise (at 30 Hz) and power frequency (at 50 Hz). The desired EMG signal was obtained with a band-pass filter with cutoff frequencies of 20 Hz and 450 Hz. The EMG traces from all tasks were segmented into three stages of 4 s each. Recognizing the stochastic nature of EMG signals, we employed an analysis window rather than relying on instantaneous values [33]. A 100 ms fixed-width sliding window featuring a 50% overlap (205 samples per window, totaling 40 windows) was used to calculate the time-domain features for each stage.

The IMU sensor recorded 3-dimensional acceleration and gyroscopic data at a frequency of 100 Hz. Each stage of the task had a total duration of 4 s, accumulating 400 samples. To make the IMU data consistent with the EMG data, these 400 samples were divided into 40 non-overlapping windows containing 10 samples to obtain average values. All the data were organized systematically so that for each participant, there were 3600 data points (40 windows x 5 orientations x 2 limbs x 3 stages x 3 trials) of EMG and IMU data. Unfortunately, because of a reduction in kinematic data readings from the IMU sensor for two participants, the corresponding EMG data had to be omitted. All data processing was carried out using the MATLAB R2021a software (The Math Works Inc., 2021).

E. MACHINE LEARNING AND FEATURE SELECTION

In this study, a comparative analysis of three classifiers is conducted to develop robust machine learning (ML) models. SVM [34], KNN [35], and ES [36] classifiers are chosen for their widespread usage in EMG signal classification across various applications, especially in neuromuscular and rehabilitation research. Through evaluating SVM, KNN, and ES classifiers, we aim to identify the optimal classifiers for our ML task.

It is essential to identify the most discriminating features from the sensor data prior to applying sensor fusion and ML classification. The six IMU features included were: three accelerations, i.e., the mean acceleration in the x-axis (mAccX), y-axis (mAccY), and z-axis (mAccZ) direction; and three angular rotations, i.e., the mean rotation about the x-axis (mGyrX), y-axis (mGyrY), and z-axis (mGyrZ). For EMG data, the time domain features demonstrate a greater degree of consistency in performance over an extended duration, and allow simple computation, low time consumption compared to other domains, and better prediction accuracy in clinical and rehabilitation applications [37], [38], [39]. Table 1 lists fifteen (15) EMG time domain features, along with their mathematical equations, that were extracted from each muscles' EMG signal [39], [40]. This resulted in a 60-feature vector of EMG data. For feature reduction, the wrapper method was applied to select the features having the greatest effect on recognition. Each of the fifteen EMG features from all four muscles were used for classification of movement via our selected classifiers of ES, KNN, and SVM. Table 1 also lists the accuracies obtained for each feature with each of the three classifiers, as well as their average

TABLE 1. EMG feature reduction with wrapper method. The names of 15 features along with their mathematical equations are given. The accuracies obtained for them with the three classifiers support vector machine (SVM), k-nearest neighbors (KNN), and ensemble (ES) are shown. The five features that had the highest average accuracies were selected, as shown in bold. Abbreviations: enhanced mean absolute value (EMAV), enhanced waveform length (EWL), zero crossing (ZC), slope sign change (SSC), root mean square (RMS), average amplitude change (ACC), difference absolute standard deviation value (DASDV), log detector (LG), modified mean absolute value 1 (MMAV1), modified mean absolute value 2 (MMAV2), myopulse percentage rate (MYOP), simple square integral (SSI), variance of EMG (VAR), Willison amplitude (WA), and maximum fractal length (MFL).

S. No	Features	Equations	Accuracy			Average Accuracy of Three Classifiers (%)
			SVM (%)	KNN (%)	ES (%)	
1	**EMAV**	$\frac{1}{N}\sum_{i=1}^{N}\lvert(x_i)^p\rvert$ $p=\begin{cases}0.75, 0.2N \le i \le \\ 0.5, otherwi\end{cases}$	**49.4**	**49.6**	**51.5**	**50.16**
2	**EWL**	$\frac{1}{N}\sum_{i=1}^{N}\lvert(x_{i+1}-x_i)^p\rvert$ $p=\begin{cases}0.75, 0.2N \le i \le \\ 0.5, otherwi\end{cases}$	**51.9**	**52.0**	**50.7**	**51.53**
3	ZC	$\sum_{i=1}^{N-1}[sgn(x_i * x_{i+1}) \cap \lvert x_i - x_{i+1}\rvert] \ge threshold,$ $sign(x)=\begin{cases}1, x \ge threshold\\0, x \le threshold\end{cases}$	38.9	41.1	36.9	39.06
4	SSC	$\sum_{i=2}^{N-1}\lvert f[(x_{i+1}-x_i) * (x_{i-1}-x_i)]\rvert,$ $f(x)=\begin{cases}1, x \ge threshold\\0, x < threshold\end{cases}$	40.2	42.4	42.0	41.5
5	RMS	$\sqrt{\frac{1}{N}\sum_{i=1}^{N}x_i^2}$	46.9	48.5	48.3	47.9
6	**AAC**	$\frac{1}{N}\sum_{i=1}^{N-1}\lvert x_{i+1}-x_i\rvert$	**51.7**	**51.7**	**48.9**	**50.76**
7	**DASDV**	$\sqrt{\frac{1}{N-1}\sum_{i=1}^{N-1}(x_{i+1}-$	**52.0**	**51.9**	**49.4**	**51.1**
8	LD	$exp\left(\frac{1}{N}\sum_{i=1}^{N}log(\lvert x_i\rvert)\right)$	48.3	47.0	50.4	48.56
9	MMAV1	$\frac{1}{L}\sum_{i=1}^{N}w_i * \lvert x_i\rvert,$ $w_i=\begin{cases}1, 0.25N \le i \le 0.\\0.5, others\end{cases}$	47.2	47.2	52.4	48.93
10	MMAV2	$\frac{1}{L}\sum_{i=1}^{N}w_i * \lvert x_i\rvert,$ $w_i=\begin{cases}1, 0.25N \le i \le 0.\\\frac{4i}{N}, i < 0.25N\\\frac{4(i-N)}{N}, otherv\end{cases}$	46.7	47.4	51.7	48.6
11	MYOP	$\frac{1}{N}\sum_{i=1}^{N}f(\lvert x_i\rvert),$	29.1	33.0	32.5	31.53

TABLE 1. *(Continued.)* EMG feature reduction with wrapper method. The names of 15 features along with their mathematical equations are given. The accuracies obtained for them with the three classifiers support vector machine (SVM), k-nearest neighbors (KNN), and ensemble (ES) are shown. The five features that had the highest average accuracies were selected, as shown in bold. Abbreviations: enhanced mean absolute value (EMAV), enhanced waveform length (EWL), zero crossing (ZC), slope sign change (SSC), root mean square (RMS), average amplitude change (ACC), difference absolute standard deviation value (DASDV), log detector (LG), modified mean absolute value 1 (MMAV1), modified mean absolute value 2 (MMAV2), myopulse percentage rate (MYOP), simple square integral (SSI), variance of EMG (VAR), Willison amplitude (WA), and maximum fractal length (MFL).

		$f(x)=\begin{cases}1, x \ge threshold\\0, x < threshold\end{cases}$				
12	SSI	$\sum_{i=1}^{N}x_i^2$	48.9	47.8	51.1	49.2
13	VAR	$\frac{1}{N-1}\sum_{i=1}^{N}x_i^2$	47.6	46.7	51.7	48.6
14	WA	$\sum_{i=2}^{N}f(\lvert x_i\rvert),$ $f(x)=\begin{cases}1, x \ge threshold\\0, x < threshold\end{cases}$	36.1	35.9	35.7	35.9
15	**MFL**	$log_{10}\sqrt{\sum_{i=1}^{N-1}(x_{i+1}-x}$	**52.4**	**54.8**	**51.5**	**53.0**

accuracies. The features yielding an average accuracy of greater than 50% across the three classifiers were chosen to be used in sensor fusion. The five selected features selected from the wrapper method were enhanced mean absolute value, enhanced waveform length, average amplitude change, difference absolute standard deviation value, and maximum fractal length. The sensor fusion methodology consisted of incorporating these five EMG features for each of the four muscles and the six IMU features, resulting in a 26-feature vector for classification.

F. CLASSIFICATION

A supervised ML approach was used to identify the patterns within the IMU and EMG data for 30 different trunk movements using the 26-feature sensor fusion vector. Figure 3 shows the ML models for the three-level classification performed in order to obtain a better overall accuracy [25]. Each level of classification represents a unique aspect of the movement, while together, the levels in can identify the complete seated trunk movement. The first level determines the stage of the trunk movement, and classifies data into the three stages, Extend, Reach, and Return, using the Ex/Re/Rt model. The second level determines the choice of upper limb during the movement; therefore, the data is further categorized into right or left upper limb movement using the Ex-R/L, Re-R/L, and Rt-R/L models for the Extend, Reach, and Return stages, respectively. The third level determines the orientation of the movement, using six-ML models to classify the data into orientations of 0°, 45°, 90°, 135°, and 180°. All of the ten models in the three levels were trained with each of the three ML classifiers (ES, KNN, and SVM)

to obtain the optimum model exhibiting best classification accuracy.

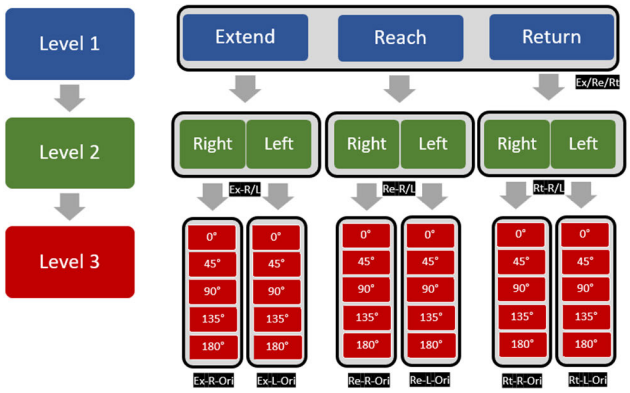

FIGURE 3. The three-level classification system. Level 1 classifies motions into stages of extend, reach, and return; and has one model. Level 2 distinguishes between movements with the right or left upper limbs; and has three models. Level 3 categorizes each movement into five orientations; and has six models. The name of each model is highlighted in black.

To evaluate the classification performance of these models, confusion matrices were used to depict the actual and predicted classification results obtained with the three classifiers. The total dataset was segregated as 80% for training the ML models and 20% for testing the best performing models. To reduce overfitting in training the ML models, a five-fold cross-validation method was used on the training dataset using the Classification Learner App in MATLAB. The models were trained to refine their performance and identify the optimal combination of hyperparameters to minimize classification errors. The performance metrics obtained for all ML algorithms were accuracy, precision, recall, and F1 score metrics, computed according to equations (1), (2), (3), and (4), respectively. These metrics are averaged over the five folds of training data subsets and are associated with true positives (TP), false positives (FP), true negatives (TN), and false negatives (FN).

$$Accuracy = \frac{TP + TN}{TP + FP + FN + TN} \times 100\% \quad (1)$$

$$Precision = \frac{TP}{TP + FP} \quad (2)$$

$$Recall = \frac{TP}{TP + FN} \quad (3)$$

$$F1\ score = 2 \times \frac{precisionxrecall}{precision + recall} \quad (4)$$

In these equations, Accuracy is the comprehensive classification rate, assessing how effectively the classifier predicts classes; Precision is the rate of accurately predicted classes; and Recall is the proportion of correctly categorized positive classes. The F1 score is the harmonic mean of precision and recall, scaled by 2. This metric is particularly useful for assessing prediction quality in scenarios with imbalanced class distributions.

III. RESULTS

A. MODELS FOR THREE-LEVEL CLASSIFICATION

The models constructed in this study exhibited high levels of accuracy, with average accuracies among the best-performing ML classifiers being 90.89% for level 1, 98.53% for level 2, and 96.90% for level 3. The average accuracy among all ten models of all levels comes to 95.44%.

Figure 4 shows heatmaps for the four metrics obtained for each of the three classifiers for each of the ten models. The columns in heatmaps represent the classifier used, while the rows represent each model. The color bar on the right side gives the scale of the colors. A darker color represents a higher metric value. The scale for ''Accuracy'' goes from 88% to 100%, while it is from 0.88 to 1.0 for the rest.

In the Level 1 classification, the Extend, Reach, and Return stages are distinguished through model Ex/Re/Rt. The KNN produced the best metrics for this model, with the precision, recall, and F1 score metrics of 0.909. Figure 5 shows the confusion matrix for this classification. The values along the diagonal are the true positive rates (TPR), and the sums of the misclassifications in each row are the false negative rates (FNR). The color bar gives the range of colors for values from 0 to 100%. The level 1 model had a TPR of 88.84% for Extend, 95.06% for Reach, and 88.76% for Return. Notably, the misclassification rates were lowest for the Reach stage, with an FNR of 4.943% (3.915% + 1.028%), followed by 11.155% for the Extend stage and 11.238% for the Return stage.

In the Level 2 classification, the movements of the right or left upper limb were distinguished. Therefore, we had three models at this level that represented the further classification of movements in Extend, Reach, and Return stages as models Ex-R/L, Re-R/L, and Rt-R/L, respectively. All three classifiers had excellent accuracies that are very close, however, ES had the best metrics of all three models. The best accuracies achieved were 97.85% for model Ex-R/L, 98.93% for model Re-R/L, and 98.81% for model Rt-R/L. Their precision, recall, and F1 scores were the same across the models, i.e., 0.979 for model Ex-R/L, 0.989 for model Re-R/L, and 0.988 for model Rt-R/L. Figure 6 shows the confusion matrices of this level, where Ex-R/L effectively achieved TPRs of 98.1% and 97.59%, with misclassifications represented by FNRs of 1.902% and 2.41% for the right and left limbs, respectively. Likewise, model Re-R/L attained TPRs of 99.33% and 98.54%, with misclassifying represented by FNRs of 0.6684% and 1.46% for the right and left limb, respectively. Lastly, for the Return stage model Rt-R/L, the TPRs were 98.88% and 98.75%, with misclassifications represented by FNRs of 1.123% and 1.251% for the right and left limbs, respectively.

In the Level 3 classification, the five orientations were distinguished as 0°, 45°, 90°, 135°, and 180°. Since there were three stages and two upper limb cases, this led to six combinations, and therefore, we had six classification models at this level. The Ex-R-Ori, Ex-L-Ori, Re-R-Ori, Re-L-Ori, Rt-R-Ori, and Rt-L-Ori models achieved highest accuracies

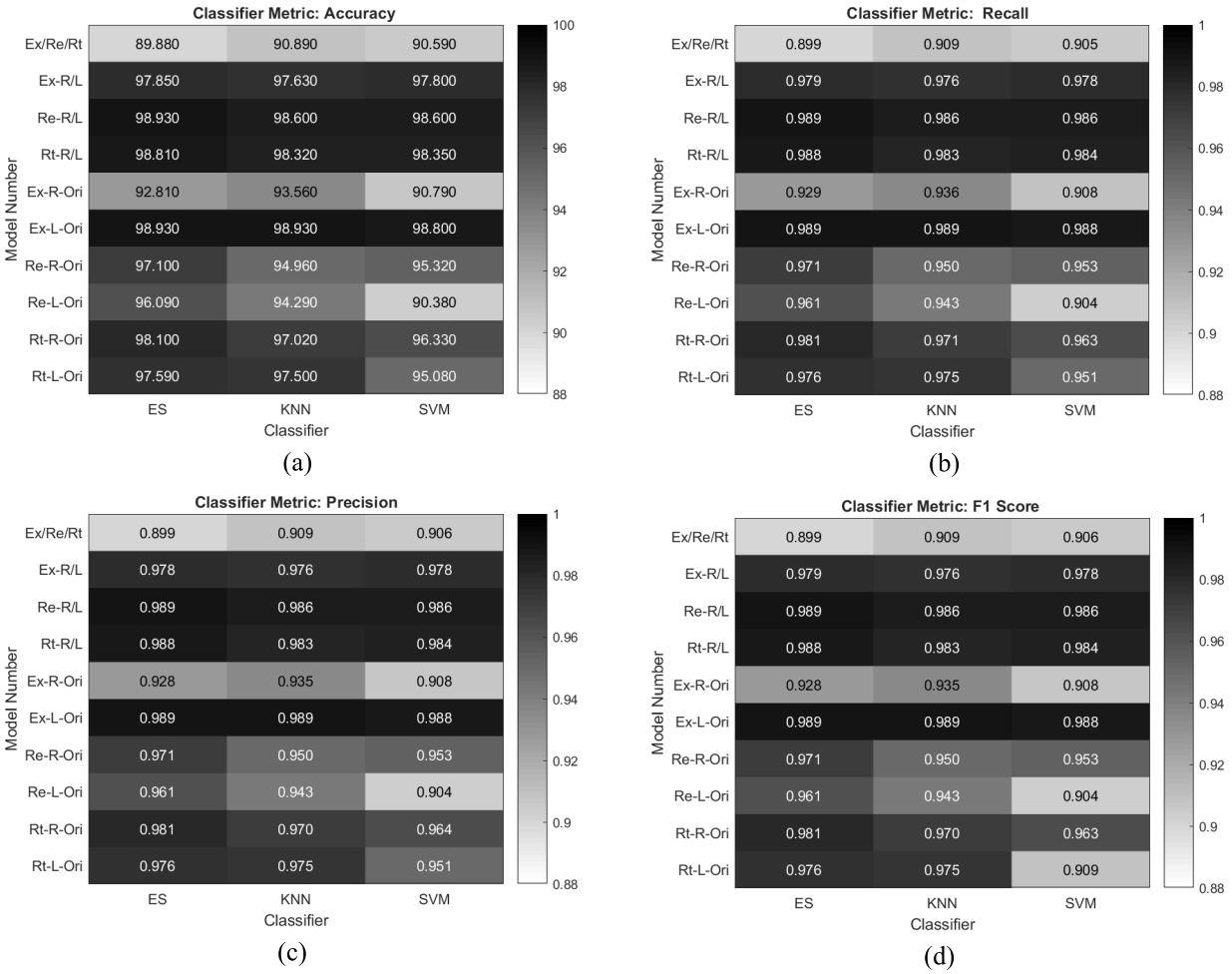

FIGURE 4. Heat maps of classification metrics for all ten models for each of the three classifiers: (a) accuracy, (b) recall, (c) precision, and (d) F1 Score.

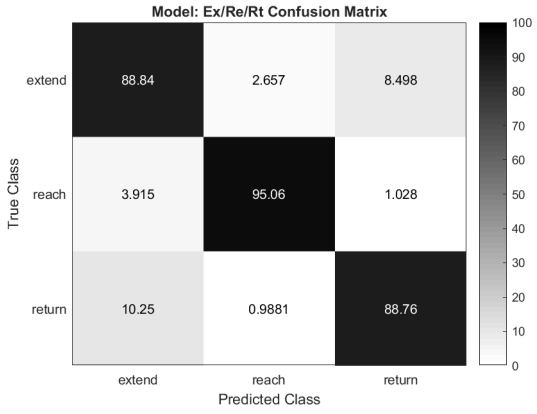

FIGURE 5. Level 1 confusion matrix for Ex/Re/Rt model with SVM classifier. The color bar range is 0 to 100%.

of 93.56%, 98.93%, 97.10%, 96.09%, 98.10%, and 97.59%, respectively. Model Ex-R-Ori had the best performance with KNN, while model Ex-L-Ori had a tie between ES and KNN. The remaining models had the best performance with the ES classifier.

The precisions, recall, and F1 scores were the same across the models as 0.935, 0.989, 0.971, 0.961, 0.981, and 0.976 for models Ex-R-Ori, Ex-L-Ori, Re-R-Ori, Re-L-Ori, Rt-R-Ori, and Rt-L-Ori, respectively. Figure 7 shows the confusion matrices of all the level 3 models, where the color bar represents the color range of 0 to 100% for each model.

B. CASCADED CLASSIFICATION

The cascaded classification refers to the utilization of the three-level classification system, as depicted in Figure 3, in order to fully identify the seated trunk movement. The ten selected models having highest individual accuracies are put together to test the data classification accuracy. Table 2 shows the hyperparameters of the ten selected models along with their relevant parameters. Two models used KNN, while the other eight models used ES.

The testing was done using the initially segregated 20% testing data from the original dataset. Thus, testing is done on new data that is not used in training. In cascaded

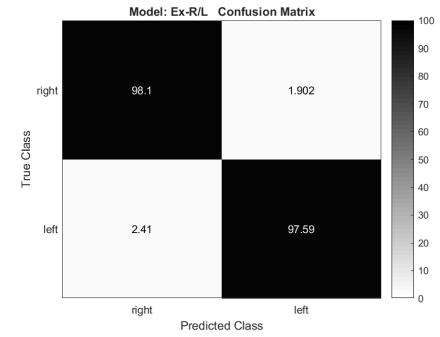

(a)

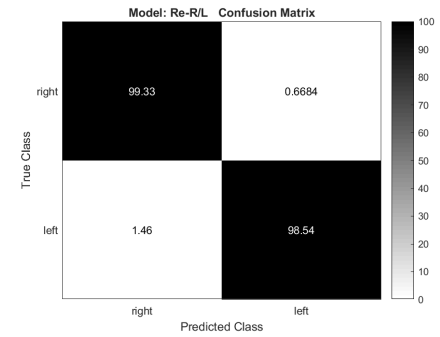

(b)

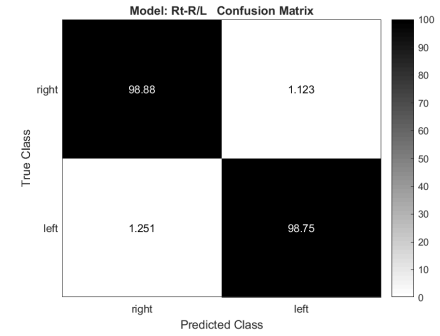

(c)

FIGURE 6. Level 2 confusion matrices for models (a) Ex-R/L, (b) Re-R/L, and (c) Rt-R/L. Each model used the ES classifier. The color bar range is 0 to 100%.

classification, all data passes through three models, i.e., one in each level of classification. Level 1 is comprised of a single model; therefore, every data passes this model. Based on the classification output of level 1 model, the data passes through one of the level 2 models. Similarly, based on classification output in level 2, the data passes through one of the level 3 models. Finally, the movement is identified based on the classification outputs of all three levels.

The overall accuracy achieved in the cascaded classification was found to be 87.0%. Figure 8 shows the confusion matrix for cascaded classification. The vertical and horizontal lines separate the stages for better understanding. The boxes in the diagonal of the figure show the true classification, whereas other boxes represent misclassifications. Misclassifications that form diagonal pattern, show stage misclassifications, while those close to the central diagonal result from orientation misclassification.

TABLE 2. Hyperparameter settings for various classification models.

MODEL	CLASSIFIER	HYPERPARAMETERS			
		Ensemble Method	No. of Max. Split	No. of Learners	No. of Neighbor
Ex/Re/Rt	KNN				10
Ex-R/L	ES	Gentle Boost	4778	270	
Re-R/L	ES	Gentle Boost	133	479	
Rt-R/L	ES	Gentle Boost	5918	291	
Ex-R-Ori	KNN				7
Ex-L-Ori	ES	Bag	6555	484	
Re-R-Ori	ES	Adaboost	284	448	
Re-L-Ori	ES	Bag	2368	496	
Rt-R-Ori	ES	Bag	18185	489	
Rt-L-Ori	ES	Bag	5412	339	

IV. DISCUSSION

The present study aimed to develop a system for automatically detecting motion intention in seated individuals utilizing a trunk orthosis CMPTO. EMG and IMU sensor data were used to represent muscle activity and motion kinematics, respectively. The findings of this study have promising implications for the development and implementation of an active orthosis for enhancing seated trunk movements and preventing falls.

A. PERFORMANCE OF MODELS

A comprehensive ML approach was adapted in this study, from the selection of suitable data features to the selection of suitable classifier with sensor fusion, and finally, the cascading of models to develop a seated trunk movement detection system. The models constructed in this study achieved high levels of accuracy, with performance metrics comparable to those observed in previous studies [18], [26]. The ES was the most common classifier with the best performance metrics. Similar findings are reported in tremor identification study on patients [41]. Interestingly, all level 2 models used the same ES classifier. Among the ES classifiers, both bagging and boosting methods performed well individually without combining with any other classifiers [36]. Comparing KNN and SVM, we note that using higher k values, as in our case, leads to better performance of KNN [35], whereas the opposite is true for lower k values [26].

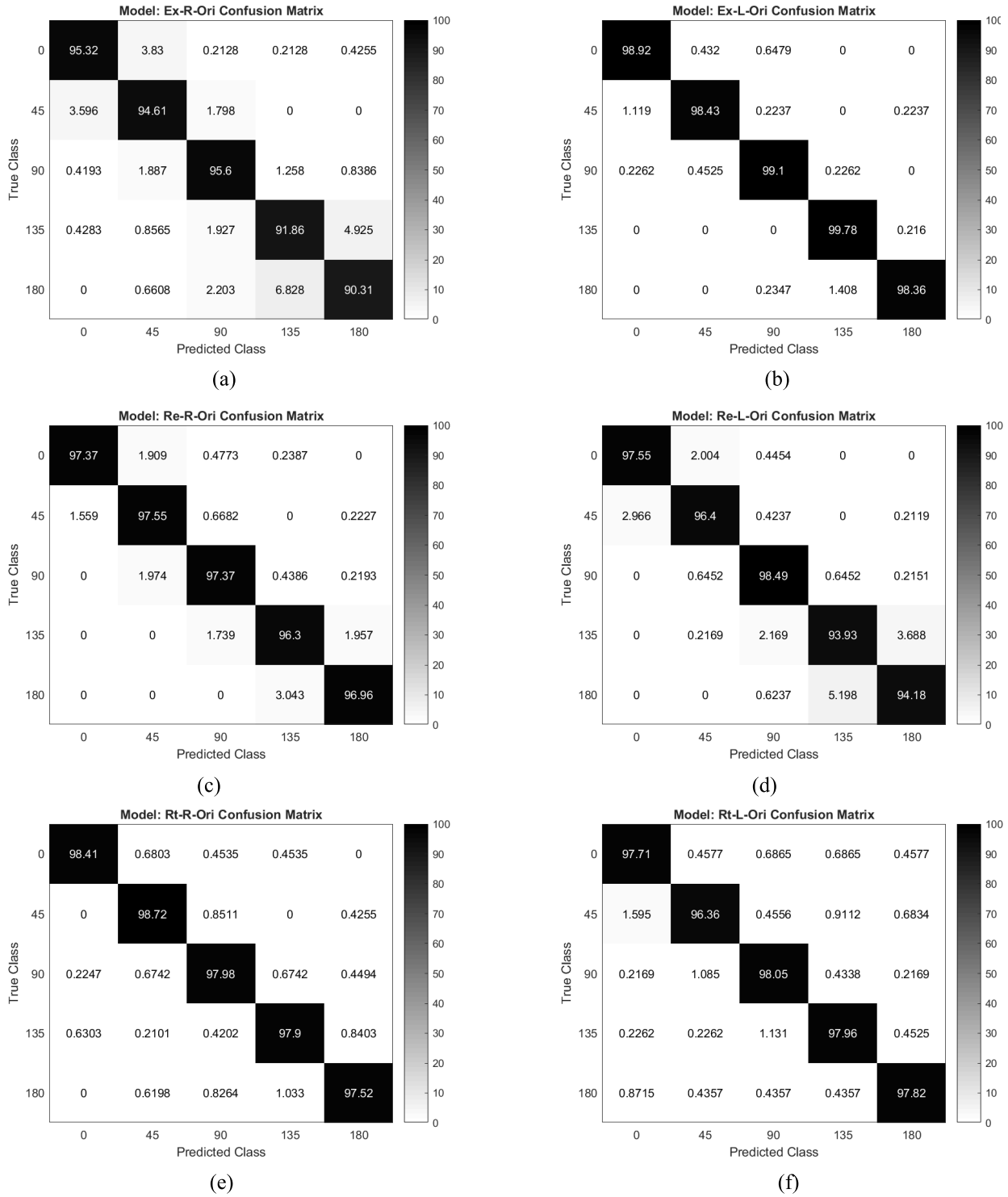

FIGURE 7. Level 3 confusion matrices for models (a) Ex-R-Ori with KNN, (b) Ex-L-Ori with SVM, (c) Re-R-Ori with ES, (d) Re-L-Ori with ES, (e) Rt-R-Ori with ES, and (f) Rt-L-Ori with ES classifiers. The color bar range is 0 to 100%.

Classification accuracies are known to decrease when there are numerous classes to be distinguished [42]. Therefore, the ML models were divided into a three-level classification scheme. Level 1 classification is differentiated among degrees of trunk movement. Level 2 classification identified the upper limb used in the movement, as the trunk rotation is different depending on the movement done by either upper limb at different degrees [43]. Level 3 classification identified the orientation of the movement and was important to encompassing a wide reachable workspace.

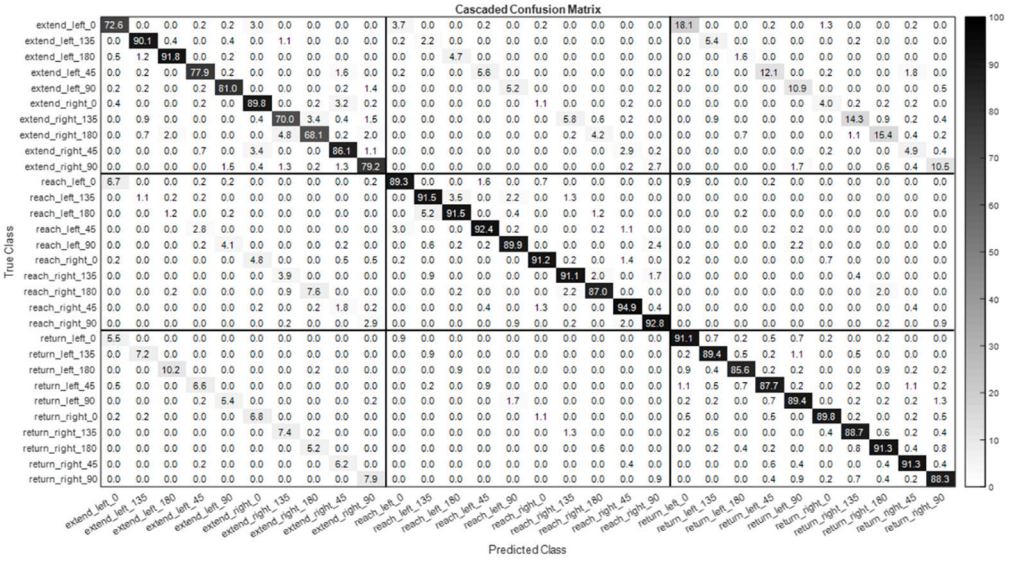

FIGURE 8. The confusion matrix obtained for the cascaded classification to predict the 30 trunk movements. The horizontal and vertical lines separate the stages in true and predicted class, respectively. The number in each cell represents the accuracy percentage for prediction. The color bar range is 0 to 100%.

Interestingly, the classification accuracies did not depend on the number of classes in the classifier models. Among the three levels, the highest accuracies were seen in Level 2, followed by Level 3 and Level 1, where the number of classes were two, five, and three, respectively. Moreover, the Level 2 classification had the highest accuracy in the model for the Reach stage, followed by the Return, and Extend stages. This difference may be because, as the trunk muscle activity varies with the nature of the task [44], higher muscle activity is expected for the Reach stage because of its fatiguing nature [32]. This could have led to more distinct feature values in this stage, and therefore, the highest accuracy. This also suggests that spectral features of EMG, which change with fatigue, should also be considered to improve classification accuracy [16].

We classified 30 trunk movements with a cascaded scheme for a trunk motion intention detection system incorporating ten individual models. While this cascaded system yielded commendable accuracy, it is essential to address a few areas of misclassification. Some misclassifications were observed in adjacent orientations. This could be due to an overlap in the training data, as highly similar postures make it challenging to separate overlapping in the feature space [45]. In addition, participants with different body mass indices may have had different strategies for movements [46]. As a result, some adjacent movements may have had very similar feature values that led to ambiguity in detecting the intended orientation.

Motion assistance can take into account user demographics so that customized support is made available for people with varying degrees of trunk stability [47]. Moreover, incorporating frequency and time-frequency domain features for EMG analysis can capture spectral characteristics and provide robust classification of dynamic movements. These features can also recognize muscle fatigue from changes in frequency content over time [48]. Additional optimization techniques such as data scaling may enhance accuracies for SVM and KNN [49]. Furthermore, deep learning techniques have been proven to achieve high classification accuracies [50]. Therefore, these techniques could be used for feature engineering and selection to extract relevant trunk movement intention information from EMG and IMU data in future studies.

Similar to our findings, the sensor fusion combining IMU and EMG sensor data for prediction has also been applied to motion intention detection of lower limb movement and gait, achieving classification accuracies above 90% [51], [52], [53]. It can be argued that some gait analysis studies used a single IMU [54] whereas we have used two sensors, however, it is important to note that unlike human gait, seated trunk movement is not cyclical. Consequently, the symmetric seated movements can be challenging to distinguish with a single IMU sensor. Moreover, even though the gait studies have used a single sensor for movement identification, there is little consensus on the optimum location of sensor placement. On the contrary, considering the segmental trunk movement [55], the ideal IMU sensor location for seated trunk movement is further from the base (seat).

B. ENHANCING SAFETY AND INDEPENDENCE

This study introduces the concept of an active trunk orthosis that could be designed for wheelchair users to assist in their seated daily life activities. The incorporation of a machine learning framework can recognize the motion intention of users and provide real-time adjustment of assistance during movements [56]. The development of this promising technology has the potential to prevent falls, improve stability, and

user autonomy, thereby enhancing the quality of life for those with compromised trunk control [57]. This paves the way for future assistive technologies that can adapt in real-time to the unique requirements of users, potentially improving efficacy and user satisfaction. Future design iterations could incorporate additional measurements such as seating pressure to allow users to perform a broader range of activities with greater ease. Additionally, future developments could focus on further refining the predictive capabilities of machine learning algorithms to anticipate and mitigate potential risks in real-time, thereby reducing the likelihood of accidents and injuries.

C. LIMITATION OF THE STUDY

In order to facilitate controlled experimentation and validation of our framework, the study involved participants without trunk movement impairment. This approach allowed for rigorous testing and validation of our system. However, it is important to emphasize that while our results offer valuable insights and proof-of-concept, further validation with individuals who have trunk impairment is warranted. Such validation would enhance the robustness and applicability of our system in clinical settings, ensuring its effectiveness across diverse user populations.

Our study primarily focused on identifying thirty horizontal plane seated trunk movements. While these were more than those identified previously, future studies could further strengthen our findings by including movements in additional planes, particularly targeting tasks at varying heights. Furthermore, considering daily activities that involve combinations of movements across different planes would be beneficial for validating the machine learning models developed in this study. This expansion would not only enhance the comprehensiveness of our approach but also increase the applicability of our findings to a wider range of real-world scenarios.

Finally, future studies can expand the patient demographics and incorporate it in developing the ML models. This can enable the classification system to additionally determine personalized assistance based on the user's specific needs and abilities for performing trunk movements in various postures.

V. CONCLUSION

The study made substantial progress toward the development of an active orthosis for individuals with unstable trunk control. The incorporation of EMG and IMU data, along with a unique three-level classification system, yielded promising results. Further research in feature selection and model optimization has the potential to enhance outcomes, fostering greater independence and well-being for wheelchair users. This work lays a strong foundation for future assistive technology in trunk rehabilitation.

ACKNOWLEDGMENT

The authors extend their appreciation to the King Salman Center for Disability Research for funding this work through Research Group no KSRG-2023-299.

REFERENCES

[1] S. E. Sonenblum, S. H. Sprigle, J. S. Martin, and PE, "Everyday sitting behavior of full-time wheelchair users," *J. Rehabil. Res. Develop.*, vol. 53, no. 5, pp. 585–598, 2016, doi: 10.1682/jrrd.2015.07.0130.

[2] E. Linder-Ganz, M. Scheinowitz, Z. Yizhar, S. S. Margulies, and A. Gefen, "How do normals move during prolonged wheelchair-sitting?" *Technol. Health Care*, vol. 15, no. 3, pp. 195–202, May 2007, doi: 10.3233/thc-2007-15303.

[3] J. V. G. Robertson and A. Roby-Brami, "The trunk as a part of the kinematic chain for reaching movements in healthy subjects and hemiparetic patients," *Brain Res.*, vol. 1382, pp. 137–146, Mar. 2011, doi: 10.1016/j.brainres.2011.01.043.

[4] L. Abou and L. A. Rice, "The associations of functional independence and quality of life with sitting balance and wheelchair skills among wheelchair users with spinal cord injury," *J. Spinal Cord Med.*, pp. 1–8, Apr. 2022, doi: 10.1080/10790268.2022.2057721.

[5] E. T.-H. Chu and K.-J. Chen, "SWAF: Smart wheelchair for fall risk assessment," *J. Syst. Archit.*, vol. 131, Oct. 2022, Art. no. 102694, doi: 10.1016/j.sysarc.2022.102694.

[6] W. Tse, L. S. Libow, R. Neufeld, G. Lesser, J. Frank, S. Dolan, C. Tarshish, J.-M. Gracies, C. W. Olanow, W. C. Koller, and T. D. Hälbig, "Prevalence of movement disorders in an elderly nursing home population," *Arch. Gerontol. Geriatrics*, vol. 46, no. 3, pp. 359–366, May 2008, doi: 10.1016/j.archger.2007.05.008.

[7] U. Granacher, A. Gollhofer, T. Hortobágyi, R. W. Kressig, and T. Muehlbauer, "The importance of trunk muscle strength for balance, functional performance, and fall prevention in seniors: A systematic review," *Sports Med.*, vol. 43, no. 7, pp. 627–641, Jul. 2013, doi: 10.1007/s40279-013-0041-1.

[8] Q. Nie, L. Rice, J. Sosnoff, and W. Rogers, "Investigating falls and rehabilitation use in older wheelchair users from the national health and aging trends study," *Innov. Aging*, vol. 4, no. 1, pp. 906–907, Dec. 2020, doi: 10.1093/geroni/igaa057.3335.

[9] B. S. Lin, "The impact of aging and reaching movements on grip stability control during manual precision tasks," *BMC Geriatr.*, vol. 21, no. 1, pp. 1–12, Dec. 2021, doi: 10.1186/s12877-021-02663-3.

[10] L. H. C. Peeters, I. Kingma, J. H. van Dieën, and I. J. M. de Groot, "Don't forget the trunk in Duchenne muscular dystrophy patients: More muscle weakness and compensation than expected," *J. NeuroEng. Rehabil.*, vol. 16, no. 1, p. 44, Dec. 2019, doi: 10.1186/s12984-019-0515-y.

[11] S. Kato, S. Demura, Y. Kurokawa, N. Takahashi, K. Shinmura, N. Yokogawa, N. Yonezawa, T. Shimizu, R. Kitagawa, and H. Tsuchiya, "Efficacy and safety of abdominal trunk muscle strengthening using an innovative device in elderly patients with chronic low back pain: A pilot study," *Ann. Rehabil. Med.*, vol. 44, no. 3, pp. 246–255, Jun. 2020, doi: 10.5535/arm.19100.

[12] J. Katsuhira, K. Matsudaira, H. Oka, S. Iijima, A. Ito, T. Yasui, and A. Yozu, "Efficacy of a trunk orthosis with joints providing resistive force on low back load during level walking in elderly persons," *Clin. Interventions Aging*, vol. Volume 11, pp. 1589–1597, Nov. 2016, doi: 10.2147/cia.s108033.

[13] D. Li, E. Q. Yumbla, A. Olivas, T. Sugar, H. B. Amor, H. Lee, W. Zhang, and D. M. Aukes, "Origami-inspired wearable robot for trunk support," *IEEE/ASME Trans. Mechatronics*, vol. 28, no. 3, pp. 1466–1476, Jun. 2023, doi: 10.1109/TMECH.2022.3220136.

[14] Y. Kurokawa, S. Kato, S. Demura, K. Shinmura, N. Yokogawa, N. Yonezawa, T. Shimizu, R. Kitagawa, H. Miaki, and H. Tsuchiya, "Validation and comparison of trunk muscle activities in male participants during exercise using an innovative device and abdominal bracing maneuvers," *J. Back Musculoskeletal Rehabil.*, vol. 35, no. 3, pp. 589–596, May 2022, doi: 10.3233/bmr-210001.

[15] A. N. Aicha, G. Englebienne, K. van Schooten, M. Pijnappels, and B. Kröse, "Deep learning to predict falls in older adults based on daily-life trunk accelerometry," *Sensors*, vol. 18, no. 5, p. 1654, May 2018, doi: 10.3390/s18051654.

[16] A. Moniri, D. Terracina, J. Rodriguez-Manzano, P. H. Strutton, and P. Georgiou, "Real-time forecasting of sEMG features for trunk muscle fatigue using machine learning," *IEEE Trans. Biomed. Eng.*, vol. 68, no. 2, pp. 718–727, Feb. 2021, doi: 10.1109/TBME.2020.3012783.

[17] P. Xu, D. Xia, B. Zheng, L. Huang, and L. Xie, "A novel compensatory motion detection method using multiple signals and machine learning," *IEEE Sensors J.*, vol. 22, no. 17, pp. 17162–17172, Sep. 2022, doi: 10.1109/JSEN.2022.3190503.

[18] S. Cai, G. Li, S. Huang, H. Zheng, and L. Xie, "Automatic detection of compensatory movement patterns by a pressure distribution mattress using machine learning methods: A pilot study," *IEEE Access*, vol. 7, pp. 80300–80309, 2019, doi: 10.1109/ACCESS.2019.2923077.

[19] S. Rothstock, H. R. Weiss, D. Krueger, and L. Paul, "Clinical classification of scoliosis patients using machine learning and markerless 3D surface trunk data," *Med. Biol. Eng. Comput.*, vol. 58, no. 12, pp. 2953–2962, Dec. 2020, doi: 10.1007/s11517-020-02258-x.

[20] W. S. Marras, "Reliability of a wearable motion system for clinical evaluation of dynamic lumbar spine function," *Adv. Complementary Alternative Med.*, vol. 7, no. 2, p. 672, Jul. 2022, doi: 10.31031/acam.2022.07.000660.

[21] M. Abdollahi, S. Ashouri, M. Abedi, N. Azadeh-Fard, M. Parnianpour, K. Khalaf, and E. Rashedi, "Using a motion sensor to categorize nonspecific low back pain patients: A machine learning approach," *Sensors*, vol. 20, no. 12, p. 3600, Jun. 2020, doi: 10.3390/s20123600.

[22] T. C. Phan, A. Pranata, J. Farragher, A. Bryant, H. T. Nguyen, and R. Chai, "Machine learning derived lifting techniques and pain self-efficacy in people with chronic low back pain," *Sensors*, vol. 22, no. 17, p. 6694, Sep. 2022, doi: 10.3390/s22176694.

[23] P. Thiry, M. Houry, L. Philippe, O. Nocent, F. Buisseret, F. Dierick, R. Slama, W. Bertucci, A. Thévenon, and E. Simoneau-Buessinger, "Machine learning identifies chronic low back pain patients from an instrumented trunk bending and return test," *Sensors*, vol. 22, no. 13, p. 5027, Jul. 2022, doi: 10.3390/s22135027.

[24] K. F. Nicholson, G. S. Collins, B. R. Waterman, and G. S. Bullock, "Machine learning and statistical prediction of fastball velocity with biomechanical predictors," *J. Biomech.*, vol. 134, Mar. 2022, Art. no. 110999, doi: 10.1016/j.jbiomech.2022.110999.

[25] P. S. Sun, D. Xu, J. Mai, Z. Zhou, S. Agrawal, and Q. Wang, "Inertial sensors-based torso motion mode recognition for an active postural support brace," *Adv. Robot.*, vol. 34, no. 1, pp. 57–67, Jan. 2020, doi: 10.1080/01691864.2019.1710381.

[26] C. Wang, X. Li, Y. Guo, R. Zhang, and W. Chen, "Classification of human movements with and without spinal orthosis based on surface electromyogram signals," *Med. Novel Technol. Devices*, vol. 16, Dec. 2022, Art. no. 100165, doi: 10.1016/j.medntd.2022.100165.

[27] E. Blasch, T. Pham, C.-Y. Chong, W. Koch, H. Leung, D. Braines, and T. Abdelzaher, "Machine learning/artificial intelligence for sensor data fusion–opportunities and challenges," *IEEE Aerosp. Electron. Syst. Mag.*, vol. 36, no. 7, pp. 80–93, Jul. 2021, doi: 10.1109/MAES.2020.3049030.

[28] L. Meng, J. Pang, Z. Wang, R. Xu, and D. Ming, "The role of surface electromyography in data fusion with inertial sensors to enhance locomotion recognition and prediction," *Sensors*, vol. 21, no. 18, p. 6291, Sep. 2021, doi: 10.3390/s21186291.

[29] J. Fu, R. Choudhury, S. M. Hosseini, R. Simpson, and J.-H. Park, "Myoelectric control systems for upper limb wearable robotic exoskeletons and exosuits—A systematic review," *Sensors*, vol. 22, no. 21, p. 8134, Oct. 2022, doi: 10.3390/s22218134.

[30] D. Wang, X. Gu, and H. Yu, "Sensors and algorithms for locomotion intention detection of lower limb exoskeletons," *Med. Eng. Phys.*, vol. 113, Mar. 2023, Art. no. 103960, doi: 10.1016/j.medengphy.2023.103960.

[31] J. Camargo, W. Flanagan, N. Csomay-Shanklin, B. Kanwar, and A. Young, "A machine learning strategy for locomotion classification and parameter estimation using fusion of wearable sensors," *IEEE Trans. Biomed. Eng.*, vol. 68, no. 5, pp. 1569–1578, May 2021, doi: 10.1109/TBME.2021.3065809.

[32] A. Z. Rao and M. A. Hasan, "Evaluation of a chair-mounted passive trunk orthosis: A pilot study on able-bodied subjects," *Sensors*, vol. 21, no. 24, p. 8366, Dec. 2021, doi: 10.3390/s21248366.

[33] L. H. Smith, L. J. Hargrove, B. A. Lock, and T. A. Kuiken, "Determining the optimal window length for pattern recognition-based myoelectric control: Balancing the competing effects of classification error and controller delay," *IEEE Trans. Neural Syst. Rehabil. Eng.*, vol. 19, no. 2, pp. 186–192, Apr. 2011, doi: 10.1109/TNSRE.2010.2100828.

[34] D. C. Toledo-Pérez, J. Rodríguez-Reséndiz, R. A. Gómez-Loenzo, and J. C. Jauregui-Correa, "Support vector machine-based EMG signal classification techniques: A review," *Appl. Sci.*, vol. 9, no. 20, p. 4402, Oct. 2019, doi: 10.3390/app9204402.

[35] I. M. Khairuddin, S. N. Sidek, A. P. P. A. Majeed, and A. A. Puzi, "Classifying motion intention from EMG signal: A k-NN approach," in *Proc. 7th Int. Conf. Mechatronics Eng. (ICOM)*, Oct. 2019, pp. 1–4, doi: 10.1109/ICOM47790.2019.8952042.

[36] E. Yaman and A. Subasi, "Comparison of bagging and boosting ensemble machine learning methods for automated EMG signal classification," *BioMed Res. Int.*, vol. 2019, pp. 1–13, Oct. 2019, doi: 10.1155/2019/9152506.

[37] C. Kendell, E. D. Lemaire, Y. Losier, A. Wilson, A. Chan, and B. Hudgins, "A novel approach to surface electromyography: An exploratory study of electrode-pair selection based on signal characteristics," *J. Neuroeng. Rehabil.*, vol. 9, no. 1, pp. 1–8, Apr. 2012, doi: 10.1186/1743-0003-9-24.

[38] A. Phinyomark, F. Quaine, S. Charbonnier, C. Serviere, F. Tarpin-Bernard, and Y. Laurillau, "EMG feature evaluation for improving myoelectric pattern recognition robustness," *Expert Syst. Appl.*, vol. 40, no. 12, pp. 4832–4840, Sep. 2013, doi: 10.1016/j.eswa.2013.02.023.

[39] J. Too. (2019). *Classification of Hand Movements based on Discrete Wavelet Transform and Enhanced Feature Extraction*. [Online]. Available: www.ijacsa.thesai.org

[40] C. Tepe and M. Erdim, "Classification of surface electromyography and gyroscopic signals of finger gestures acquired by Myo armband using machine learning methods," *Biomed. Signal Process. Control*, vol. 75, May 2022, Art. no. 103588, doi: 10.1016/j.bspc.2022.103588.

[41] X. Xing, N. Luo, S. Li, L. Zhou, C. Song, and J. Liu, "Identification and classification of parkinsonian and essential tremors for diagnosis using machine learning algorithms," *Frontiers Neurosci.*, vol. 16, Mar. 2022, Art. no. 701632, doi: 10.3389/fnins.2022.701632.

[42] P. D. Moral, S. Nowaczyk, and S. Pashami, "Why is multiclass classification hard?" *IEEE Access*, vol. 10, pp. 80448–80462, 2022, doi: 10.1109/ACCESS.2022.3192514.

[43] R. A. Preuss and M. R. Popovic, "Three-dimensional spine kinematics during multidirectional, target-directed trunk movement in sitting," *J. Electromyogr. Kinesiol.*, vol. 20, no. 5, pp. 823–832, Oct. 2010, doi: 10.1016/j.jelekin.2009.07.005.

[44] F. V. dos Anjos, M. Ghislieri, G. L. Cerone, T. P. Pinto, and M. Gazzoni, "Changes in the distribution of muscle activity when using a passive trunk exoskeleton depend on the type of working task: A high-density surface EMG study," *J. Biomech.*, vol. 130, Jan. 2022, Art. no. 110846, doi: 10.1016/j.jbiomech.2021.110846.

[45] A. Das Antar, M. Ahmed, and M. A. R. Ahad, "Challenges in sensor-based human activity recognition and a comparative analysis of benchmark datasets: A review," in *Proc. Joint 8th Int. Conf. Informat., Electron. Vis. (ICIEV) 3rd Int. Conf. Imag., Vis. Pattern Recognit. (icIVPR)*, May 2019, pp. 134–139, doi: 10.1109/ICIEV.2019.8858508.

[46] F. Berrigan, M. Simoneau, A. Tremblay, O. Hue, and N. Teasdale, "Influence of obesity on accurate and rapid arm movement performed from a standing posture," *Int. J. Obesity*, vol. 30, no. 12, pp. 1750–1757, Dec. 2006, doi: 10.1038/sj.ijo.0803342.

[47] H. Lee, Y. Choi, A. Eizad, W.-K. Song, K.-J. Kim, and J. Yoon, "A machine learning-based initial difficulty level adjustment method for balance exercise on a trunk rehabilitation robot," *IEEE Trans. Neural Syst. Rehabil. Eng.*, vol. 31, pp. 1857–1866, 2023, doi: 10.1109/TNSRE.2023.3260815.

[48] P. A. Karthick, D. M. Ghosh, and S. Ramakrishnan, "Surface electromyography based muscle fatigue detection using high-resolution time-frequency methods and machine learning algorithms," *Comput. Methods Programs Biomed.*, vol. 154, pp. 45–56, Feb. 2018, doi: 10.1016/j.cmpb.2017.10.024.

[49] M. Ahsan, M. Mahmud, P. Saha, K. Gupta, and Z. Siddique, "Effect of data scaling methods on machine learning algorithms and model performance," *Technologies*, vol. 9, no. 3, p. 52, Jul. 2021, doi: 10.3390/technologies9030052.

[50] A. Murad and J.-Y. Pyun, "Deep recurrent neural networks for human activity recognition," *Sensors*, vol. 17, no. 11, p. 2556, Nov. 2017, doi: 10.3390/s17112556.

[51] S. M. Moghadam, T. Yeung, and J. Choisne, "A comparison of machine learning models' accuracy in predicting lower-limb joints' kinematics, kinetics, and muscle forces from wearable sensors," *Sci. Rep.*, vol. 13, no. 1, p. 5046, Mar. 2023, doi: 10.1038/s41598-023-31906-z.

[52] Y. Wang, X. Cheng, L. Jabban, X. Sui, and D. Zhang, "Motion intention prediction and joint trajectories generation toward lower limb prostheses using EMG and IMU signals," *IEEE Sensors J.*, vol. 22, no. 11, pp. 10719–10729, Jun. 2022, doi: 10.1109/JSEN.2022.3167686.

[53] Y. Lu, H. Wang, F. Hu, B. Zhou, and H. Xi, "Effective recognition of human lower limb jump locomotion phases based on multi-sensor information fusion and machine learning," *Med. Biol. Eng. Comput.*, vol. 59, no. 4, pp. 883–899, Apr. 2021, doi: 10.1007/s11517-021-02335-9.

[54] A. Saboor, T. Kask, A. Kuusik, M. M. Alam, Y. Le Moullec, I. K. Niazi, A. Zoha, and R. Ahmad, "Latest research trends in gait analysis using wearable sensors and machine learning: A systematic review," *IEEE Access*, vol. 8, pp. 167830–167864, 2020, doi: 10.1109/ACCESS.2020.3022818.

[55] L. H. C. Peeters, I. J. M. de Groot, and A. C. H. Geurts, "Trunk involvement in performing upper extremity activities while seated in neurological patients with a flaccid trunk—A review," *Gait Posture*, vol. 62, pp. 46–55, May 2018, doi: 10.1016/j.gaitpost.2018.02.028.

[56] G. Giarmatzis, E. I. Zacharaki, and K. Moustakas, "Real-time prediction of joint forces by motion capture and machine learning," *Sensors*, vol. 20, no. 23, p. 6933, Dec. 2020, doi: 10.3390/s20236933.

[57] J. Sung, S. Shen, E. W. Peterson, J. J. Sosnoff, D. Backus, and L. A. Rice, "Fear of falling, community participation, and quality of life among community-dwelling people who use wheelchairs full time," *Arch. Phys. Med. Rehabil.*, vol. 102, no. 6, pp. 1140–1146, Jun. 2021, doi: 10.1016/j.apmr.2020.11.013.

AHMAD ZAHID RAO received the M.S. degree in biomedical engineering from New Jersey Institute of Technology, USA, in 2016, and the Ph.D. degree in biomedical engineering from the NED University of Engineering and Technology, Karachi, in 2022. He is currently an Assistant Professor with the NED University of Engineering and Technology. His research interests include biomechanics, rehabilitation, and assistive technology.

SABA SHAHID SIDDIQUE received the B.E. and M.S. degrees in biomedical engineering from the NED University of Engineering and Technology, Karachi, in 2020 and 2023, respectively. Her professional journey includes roles as a Biomedical Engineer with the Indus Hospital and Health Network and the Darul Sehat Hospital, Karachi. Currently, she dedicates her expertise to the field of education as a School Teacher with the Education and Literacy Department, Government of Sindh.

MUHAMMAD DANISH MUJIB received the B.E. degree in biomedical engineering from the Sir Syed University of Engineering and Technology, Karachi, Pakistan, in 2009, the M.E. degree in control and automation from Hamdard University, Karachi, in 2013, and the Ph.D. degree in biomedical engineering from the NED University of Engineering and Technology, Karachi, in 2021. He was a Senior Biomedical Engineer with the Dr. Ziauddin Hospital. He was an Assistant Professor with Hamdard University, before joining the NED University of Engineering and Technology, in 2022. His research interests include biomedical instrumentation, biosignal processing, and neuro-rehabilitation techniques using binaural beat, tDCS, and TENS.

MUHAMMAD ABUL HASAN received the Ph.D. degree in biomedical engineering from the University of Glasgow, U.K., in 2014. He is currently an Associate Professor with the Department of Biomedical Engineering, NED University of Engineering and Technology, Karachi. He is also the Co-PI of the Neurocomputation Laboratory, National Center of Artificial Intelligence, Pakistan. His research interests include neuromuscular rehabilitation, signal processing, machine learning, and artificial intelligence for cognitive enhancement (peak performance), management of psychological disorders, trunk neuromuscular stability, and pain management. He has been actively engaged in the training and development of human resources for biosignals and rehabilitation research with the NED University of Engineering and Technology.

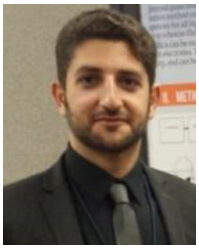

AHMAD O. ALOKAILY received the joint Ph.D. degree in biomedical engineering from New Jersey Institute of Technology and Rutgers University, USA, in 2019. He is currently an Assistant Professor of biomedical engineering with King Saud University. His research interests include neuromuscular rehabilitation, biomedical signal processing, noninvasive brain stimulation, stroke rehabilitation, neurorehabilitation, medical instrumentation, machine learning, and artificial intelligence.

TAYYABA TAHIRA received the Bachelor of Dental Surgery degree from Hamdard University, Karachi, in 2011. Subsequently, she held a fellowship in operative dentistry at the College of Physicians and Surgeons, Pakistan, in 2021. Currently, she is a Lecturer with the Dow University of Health Sciences, where she blends her passion for teaching with a commitment to staying at the forefront of healthcare advancements through integrating interdisciplinary collaboration for clinical translation. Her research interests include health professional education, education for differently abled children, biomaterials, imaging technologies, and the healthcare applications of artificial intelligence.